

Universal Nonequilibrium I - V Curve at an Interacting Impurity Quantum Critical Point

Gu Zhang,¹ Chung-Hou Chung,^{2,3,*} Chung-Ting Ke,¹ Chao-Yun Lin,² Henok Mebrahtu,¹ Alex I. Smirnov,⁴ Gleb Finkelstein,^{1,†} and Harold U. Baranger^{1,‡}

¹*Department of Physics, Duke University, Durham, North Carolina 27708-0305, U.S.A.*

²*Department of Electrophysics, National Chiao-Tung University, HsinChu, Taiwan, R.O.C.*

³*Physics Division, National Center for Theoretical Sciences, HsinChu, Taiwan, R.O.C.*

⁴*Department of Chemistry, North Carolina State University, Raleigh, North Carolina 27695, U.S.A.*

(Dated: 2 August 2017)

The nonlinear I - V curve at an interacting quantum critical point (QCP) is typically out of reach theoretically. Here, however, we provide an analytical calculation of the I - V curve at a QCP under nonequilibrium conditions and, furthermore, present experimental results to which the theory is compared. The system is a quantum dot coupled to resistive leads: a spinless resonant level interacting with an ohmic electromagnetic environment. A two channel Kondo like QCP occurs when the level is on resonance and symmetrically coupled to the leads. Using a bosonized representation, we calculate the nonlinear I - V curve at this QCP. We then show that it has a physically intuitive interpretation in terms of weak backscattering of non-interacting fermions coupled to a modified environment, thus arriving at the same I - V through dynamical Coulomb blockade theory. The agreement between our theoretical and experimental results is remarkable.

I. INTRODUCTION

Quantum phase transitions (QPT)—abrupt changes of ground state due to quantum fluctuations—are of fundamental importance in a wide variety of condensed matter many-body systems ranging from quantum materials to quantum magnets and nanostructures [1–4]. Near the quantum critical point (QCP) separating the two competing ground states, it is well established that thermodynamic observables at finite temperature show universal scaling. Properties away from equilibrium, such as when a bias is applied or a parameter suddenly changed (a quantum quench), are much less well known. However, non-equilibrium phenomena near QPT are receiving increasing attention as unanticipated features come to light [1, 5–7].

QPT occur not only in the bulk but also on the boundary of interacting systems [3] as in quantum impurity models. Nanoscale systems are ideal for studying non-equilibrium impurity QPT because of the exquisite control over parameters that they provide and the ease in creating highly non-equilibrium conditions by applying a voltage bias. The interplay between non-equilibrium and many-body effects has been studied in a variety of nanosystems through nonlinear I - V characteristics, both experimentally, for example [8–17], and theoretically, e.g. [18–30]. Indeed, analytical I - V curves have been obtained for the crossover from a QCP to a Fermi liquid state in the cases of the two-impurity and two-channel Kondo models [31–33]. At the QCP itself, however, only the exponent in the scaling regime is known: the nonequilibrium I - V characteristics at a QCP has not to our knowledge been studied either experimentally or theoretically.

Here we present both an analytical calculation of the nonequilibrium I - V curve at a QCP and experimental results

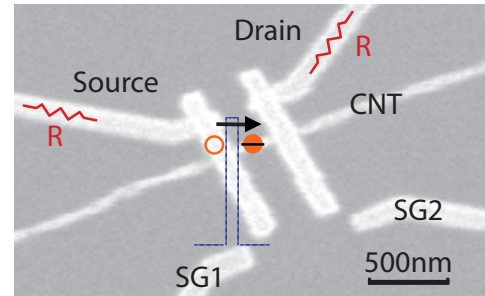


FIG. 1. Schematic of the system overlaid on a SEM image of a sample measured. A quantum dot is formed in the carbon nanotube (CNT) segment between the source and drain leads. These resistive leads create a dissipative EM environment for electrons tunneling through the dot. The tunneling barriers can be tuned with the side gates, labeled SG1 and SG2. Applying a bias between the source and drain produces a nonequilibrium state.

to which the theory can be compared in detail. The system is a spin-polarized carbon nanotube quantum dot connected to resistive leads via tunable tunnel barriers (Fig. 1). The resistive leads create an ohmic electromagnetic (EM) environment [34–36], and the quantum dot serves as the quantum impurity. The QCP occurs when a level in the dot is resonant with the leads and the dot is symmetrically coupled to them. At the QCP, the conductance through the dot at zero temperature becomes perfect (e^2/h when $T \rightarrow 0$), while otherwise it tends to zero. Several scaling relations were presented [35, 36].

Resonant tunneling in a Luttinger liquid (LL) provides considerable guidance because tunneling in an EM environment is an emulation of that system [16, 35–41]. In equilibrium, resonant peaks of perfect conductance in a LL have been studied extensively [42–50]. The QCP in this case is of the *two-channel Kondo* type, separating single-barrier (left or right) dominated weak-tunneling regimes [43, 48]. It was established that the QCP in our system is also similar to the two-channel Kondo QCP [35, 36]. Non-equilibrium properties at the LL resonant tunneling QCP, however, have not been studied.

* chung@mail.nctu.edu.tw

† gleb@phy.duke.edu

‡ baranger@phy.duke.edu

To obtain the I - V characteristics, we use a bosonized description from which an effective model near the QCP is found by duality. The correction to the perfect transmission of the QCP is given by a weak backscattering term. Treating this perturbatively to leading order in the backscattering but all orders in the coupling to the ohmic environment, we find an analytical expression for the nonlinear I - V curve at finite temperature.

We then show that this result has a simple physical interpretation, one that is not available in the corresponding LL problem. Here, modes that initially do not couple to the environment map to *non-interacting* left-moving and right-moving fermions. Indeed, at the QCP we transform to right-moving and left-moving fermionic channels between which there is weak tunneling in a modified environment. In this form, dynamical Coulomb blockade (DCB) theory [51–53] yields the same expression for the I - V curve. We close by comparing to experiment, finding excellent agreement.

II. MODEL AND HAMILTONIAN

Our system is shown in Fig. 1: a spinless resonant level between two resistive leads. The Hamiltonian in the weak-tunneling regime consists of several parts,

$$H = H_{\text{Dot}} + H_{\text{Leads}} + H_{\mu} + H_{\text{T}} + H_{\text{Env}}. \quad (1)$$

$H_{\text{Dot}} = \epsilon_d d^\dagger d$ models the dot with single energy level ϵ_d , which may be tuned by the backgate voltage V_{gate} .

$$H_{\text{Leads}} = \sum_{\alpha=S,D} \sum_k \epsilon_k c_{k\alpha}^\dagger c_{k\alpha} \quad (2)$$

represents the electrons in the source (S) and drain (D) leads, and

$$H_{\mu} = \sum_{\alpha=S,D} \sum_k \mu_{\alpha} c_{k\alpha}^\dagger c_{k\alpha} \quad (3)$$

is the chemical potential term driving the system out of equilibrium through the applied bias V , $\mu_{S/D} = \pm V/2$.

Tunneling in our system excites the electromagnetic (EM) environment through fluctuations of the voltage on the source and drain. These require a quantum description of the tunnel junction [51, 52, 54] via junction charge and phase fluctuation operators that are conjugate to each other, $\varphi_{S/D}$ and $Q_{S/D}$. A tunneling event shifts the charge on the corresponding junction, as, for example, in this contribution to tunneling from the dot to the source: $c_{kS}^\dagger e^{-i\sqrt{2\pi}\varphi_S} d$. We take the capacitance of the two tunnel junctions to be the same and so it is natural to consider the sum and difference variables $\psi \equiv (\varphi_S + \varphi_D)/2$ and $\varphi \equiv \varphi_S - \varphi_D$. The fluctuations φ involve charge flow through the system and so couple to the EM environment. In contrast, ψ is related to the total charge in the dot. Since the total charge is not coupled to the environment [51, 52, 55], we drop ψ at this point. We thus arrive at the tunnel Hamiltonian

$$H_{\text{T}} = \sum_k \left(t_S c_{kS}^\dagger e^{-i\sqrt{\frac{\pi}{2}}\varphi} d + t_D c_{kD}^\dagger e^{i\sqrt{\frac{\pi}{2}}\varphi} d + \text{h.c.} \right). \quad (4)$$

Finally, the EM environment is modeled as an ohmic bath of harmonic oscillators, represented by a bosonic field with action

$$S_{\text{Env}} = \frac{1}{2r} \int dx d\tau \left[(\partial_x \varphi)^2 + (\partial_\tau \varphi)^2 \right], \quad (5)$$

where r is the dimensionless resistance, $r \equiv Re^2/h$, and φ in Eq. (4) is $\varphi(x=0)$.

III. BOSONIZATION AT WEAK COUPLING

Our strategy is to develop a bosonized form of the weak-coupling Hamiltonian that we can then transform to strong-coupling via duality. Bosonization is possible because an impurity couples to only an effectively one-dimensional (1d) subset of lead states. We label these semi-infinite 1d leads $x \in (-\infty, 0)$ for S and $(0, +\infty)$ for D (and set their Fermi velocities equal to one). We bosonize in the standard way [42, 56], choosing the conventions of Ref. [42]:

$$c_{\alpha,L/R}^\dagger(x, t) = e^{\pm i k_F x} \frac{F_\alpha}{\sqrt{2\pi a_0}} e^{i\sqrt{\pi}[\phi_\alpha(x,t) \mp \theta_\alpha(x,t)]} \quad (6)$$

where $\alpha = S/D$ and L/R indicates left- or right-moving particles. ϕ_α and θ_α are conjugate bosonic fields that describe electronic states in the semi-infinite leads, a_0 is a short time cutoff, and F_α are Klein factors. In bosonic form $\rho_{L/R}(x) = [\pm \partial_x \phi(x) - \partial_x \theta(x)]/(2\sqrt{\pi})$ is the electron density.

Because of the sum over momentum in H_{T} , only the fields at $x = 0$ couple to the dot and environment. We can relate the fields away from the dot to their values at the origin, $\phi_{S/D}(x, \omega_n) = \phi_{S/D}(0, \omega_n) \exp(-|\omega_n x|)$ with $\omega_n \equiv 2n\pi/\beta$ the Matsubara frequency and $\beta \equiv 1/k_B T$ the inverse temperature [42, 57]. The exponential decay implies that the values at $\pm\infty$ can be ignored. Integrating over $x \neq 0$ for both the leads and the environmental field (5), we find that the effective zero-dimensional (0d) free action is

$$\frac{1}{2\beta} \sum_n |\omega_n| \left[|\phi_S(\omega_n)|^2 + |\phi_D(\omega_n)|^2 + \frac{|\varphi(\omega_n)|^2}{r} \right], \quad (7)$$

where the fields are evaluated at the origin (the x argument is dropped) and the factor $\frac{1}{2}$ results from the leads being only semi-infinite. In principle, this action could be written in terms of the conjugate fields; we use the ϕ fields since the θ fields approach zero at the dot due to their Dirichlet boundary condition at weak tunneling [42, 58]. We further define the charge and flavor fields $\phi_{c/f}(\omega_n) \equiv [\phi_S(\omega_n) \pm \phi_D(\omega_n)]/2$ in terms of which the action becomes

$$S_{\text{Leads+Env}}^{\text{eff}} = \frac{1}{\beta} \sum_n |\omega_n| \left[|\phi_c(\omega_n)|^2 + |\phi_f(\omega_n)|^2 + \frac{|\varphi(\omega_n)|^2}{2r} \right]. \quad (8)$$

Away from $x = 0$, the charge and flavor fields are [19]

$$\begin{aligned} \phi_{f/c}(x) &= \frac{1}{2} [\phi_S(-x) \mp \phi_D(x) \pm \theta_S(-x) - \theta_D(x)] \\ \theta_{c/f}(x) &= \frac{1}{2} [\pm \phi_S(-x) + \phi_D(x) + \theta_S(-x) \pm \theta_D(x)]. \end{aligned} \quad (9)$$

Note that (i) $\phi_f(x)$ is conjugate to $\theta_c(x)$ and likewise $\phi_c(x)$ to $\theta_f(x)$, and (ii) the 0d action Eq. (8) results from integrating out all $x \neq 0$ in a 1d free action in these fields.

The voltage bias in H_μ is handled using a time-dependent gauge transformation [42, 51] that moves the bias to the tunneling term—physically, when an electron hops from a lead to the dot it acquires a phase factor corresponding to the drop in bias (change in energy) across that barrier. Since the QCP occurs at symmetric coupling, we take identical coupling to the source and drain leads, $t_S = t_D \equiv t$. With symmetric tunneling and capacitance, the bias voltage drops symmetrically as well. The tunneling term is, then,

$$H_{T+\mu} = \frac{t}{\sqrt{2\pi a_0}} \left[F_S d e^{i\sqrt{\pi}\phi_c} e^{i(\sqrt{\pi}\phi_f - \sqrt{\frac{\pi}{2}}\varphi + eVt/2)} + F_D d e^{i\sqrt{\pi}\phi_c} e^{-i(\sqrt{\pi}\phi_f - \sqrt{\frac{\pi}{2}}\varphi + eVt/2)} + \text{h.c.} \right]. \quad (10)$$

$$S_{\text{Leads+Env}}^{\text{eff}} = \frac{1}{\beta} \sum_n |\omega_n| \left[|\phi_c(\omega_n)|^2 + \frac{1}{(1+r)} |\phi'_f(\omega_n)|^2 \right] + \frac{1}{(1+r)\beta} \sum_n |\omega_n| |\varphi'(\omega_n)|^2 \quad (12)$$

$$S_{T+\mu} = \int d\tau \frac{t}{\sqrt{2\pi a_0}} \left\{ F_S d e^{i\sqrt{\pi}\phi_c} e^{i(\sqrt{\pi}\phi'_f + eV\tau/2)} + F_D d e^{i\sqrt{\pi}\phi_c} e^{-i(\sqrt{\pi}\phi'_f + eV\tau/2)} + \text{c.c.} \right\}.$$

Since the field φ' completely decouples from the problem, we drop it from further consideration.

The current operator for this system is given by $\delta Z / \delta(V\tau)$ where Z is the partition function associated with the 0d action (12). One can check that it is the same as that of the original Hamiltonian, and thus transport properties of the system can be calculated from the 0d model [42].

IV. THE STRONG TUNNELING LIMIT: LINK TO A WEAK DOUBLE BARRIER

When the dot is symmetrically coupled to the leads and is exactly on resonance ($\epsilon_d = 0$), the weak-coupling description above renormalizes to a strong-coupling fixed point [35]. The system looks increasingly uniform, and the transmission goes to unity. This strong-coupling point is described by the dual to the weak-coupling effective action [42, 57, 59]. With the conjugate variables noted in Eq. 9, one finds

$$S_{\text{Leads+Env}}^{\text{eff}} = \frac{1}{\beta} \sum_n |\omega_n| \left[|\theta_f(\omega_n)|^2 + (1+r) |\theta'_c(\omega_n)|^2 \right]. \quad (13)$$

Note that this effective action describes an unconventional LL: the effective Luttinger parameter $1/(1+r)$ appears only in the θ'_c fields, leaving the θ_f field free.

As the system scales to strong coupling, two weak potential barriers become an increasingly good model for the residual effect of the quantum dot [42, 47], except for some decoupled boundary degrees of freedom that can be neglected for our purposes [60]. It is clear from Eq. (12) that the dot couples to the fields ϕ_c and ϕ'_f as if they were the true sum and difference fields of the bosonized electrons. Therefore, we take the

All fields in Eq. (10) are taken at $x = 0$, and we have used $\theta_{S/D}(0) = 0$ [42, 58] due to the Dirichlet boundary condition.

Notice that the fields $\phi_f(x = 0)$ and φ enter in the same way in Eq. (10), so we combine them via the transformation

$$\begin{aligned} \phi'_f(\omega_n) &= \phi_f(\omega_n) - \frac{1}{\sqrt{2}} \varphi(\omega_n) \\ \varphi'(\omega_n) &= \sqrt{r} \phi_f(\omega_n) + \frac{1}{\sqrt{2r}} \varphi(\omega_n). \end{aligned} \quad (11)$$

In order to combine with the free action, the Hamiltonian $H_{T+\mu}$ should be transformed to an action in imaginary time. The final expression for the action at weak coupling is

action of the symmetrical double barriers, modeled as delta functions spaced by ℓ , to be [42]

$$S_{T+\mu} = A \int d\tau \sum_{i=1,2} \cos[2\sqrt{\pi}\theta_i(\tau) + eV\tau \mp k_F\ell], \quad (14)$$

where the fields at the positions of the barriers are

$$\theta_1 \equiv \theta'_c + \theta_f \quad \text{and} \quad \theta_2 \equiv \theta'_c - \theta_f. \quad (15)$$

The strength of this double barrier term, A , is not known microscopically as it is the result of the flow from weak to strong coupling. At the end of the flow, i.e. in the limit of zero temperature and applied voltage, $A \rightarrow 0$ (see Sec. V for the renormalization analysis). The form $\cos[2\sqrt{\pi}\theta]$ appears because it corresponds to $2k_F$ backscattering of the underlying fermions [42], as can be checked by using the bosonization relation Eq. (6) to re-fermionize this term. This is, of course, the expected effect of scattering from a potential barrier. In contrast to the weak-tunneling case, we use θ fields here since ϕ fields now have Dirichlet boundary condition, becoming discretized constants at strong coupling [42, 58]. Physically, $\theta_{1/2}$ are different from the weak tunneling fields $\theta_{S/D}$ since the effect of the dissipative environment has been incorporated through θ'_c . When on resonance for a single level, one has $k_F\ell = \pi$, so that the barrier terms become

$$S_{T+\mu} = A \int d\tau \cos(2\sqrt{\pi}\theta'_c + eV\tau) \cos(2\sqrt{\pi}\theta_f). \quad (16)$$

The appearance of the bias as a phase $eV\tau$ in $S_{T+\mu}$ requires explanation: we offer three arguments. First, the combination $2\sqrt{\pi}\theta'_c + eV\tau$ in Eq. (16) is the natural duality of the way in which V is paired with ϕ'_f at weak coupling, Eq. (12).

Second, from a Landauer-Büttiker point of view [61–63], near perfect transmission the right-moving particles (from the source) have chemical potential eV higher than that of the left-moving particles (from the drain). Upon backscattering this bias should appear as a phase eVt in the backscattering operator. Thus, the bias should enter as in Eq. (14).

Our third argument for the effect of the bias at strong coupling [57, 58] considers the effect of the environment on bare bosonic fields in the weak-barrier case. Assume the system has already flowed to the strong tunneling regime with, for the moment, a dissipative free action. Then, by integrating out fields away from the impurity the 0d effective free and barrier terms are

$$\begin{aligned} S_0 &= \frac{1}{\beta} \sum_n |\omega_n| [|\theta_f(\omega_n)|^2 + |\theta_c(\omega_n)|^2] \\ &\quad + \frac{1}{\beta} \frac{1}{2r} \sum_n |\omega_n| [|\varphi(\omega_n)|^2] \\ S_T &= A \int d\tau \cos[2\sqrt{\pi}\theta_c(\tau)] \cos[2\sqrt{\pi}\theta_f(\tau)], \end{aligned} \quad (17)$$

where all the fields are evaluated at the origin. There is in addition a bias term in which both the external bias V and the fluctuating potential connected to the environmental field φ must be included. The environmental potential fluctuations are given by $\sqrt{2\pi}\dot{\varphi}$ which in a Hamiltonian formulation corresponds to the operator $eQ/(2C)$, where Q is the charge fluctuations conjugate to ϕ and C is the effective capacitance between the source and drain. In the strong coupling regime, as pointed out in the previous paragraph, the potential difference is applied between the right-moving and left-moving fermions. Thus, the bias term in Hamiltonian form is

$$\begin{aligned} H_\mu &= \frac{eV + \frac{eQ}{C}}{2} \left[\int_{-\infty}^0 dx \psi_R^\dagger(x) \psi_R(x) - \int_0^\infty dx \psi_L^\dagger(x) \psi_L(x) \right] \\ &= \frac{eV + eQ/C}{4} \frac{1}{\sqrt{\pi}} \left[\int_{-\infty}^0 dx [-\partial_x \theta_S(x) - \partial_x \phi_S(x)] \right. \\ &\quad \left. - \int_0^\infty dx [-\partial_x \theta_D(x) + \partial_x \phi_D(x)] \right] \\ &= \frac{eV + eQ/C}{4\sqrt{\pi}} [-\theta_S(0) - \theta_D(0)], \end{aligned} \quad (18)$$

where L or R represent left-moving or right-moving fermions, respectively. In order to combine with Eq. (17), we write this as an action in terms of $\theta_c(x=0, \tau)$:

$$S_\mu = - \int d\tau \left[\frac{eV}{2\sqrt{\pi}} \theta_c(\tau) + \sqrt{2} \dot{\varphi}(\tau) \theta_c(\tau) \right]. \quad (19)$$

Notice that, except for its free action, φ only couples to the θ_c field bilinearly: the potential fluctuation term can be written in terms of the Matsubara frequencies as $i\sqrt{2}\omega_n\varphi(\omega_n)\theta_c(\omega_n)$. Since it acts as an effective bias, we can integrate out the dissipation φ through a simple Gaussian path integral [58], arriving at the effective action

$$S_0 = \frac{1}{\beta} \sum_n |\omega_n| |\theta_f(\omega_n)|^2 + \frac{1+r}{\beta} \sum_n |\omega_n| |\theta_c(\omega_n)|^2. \quad (20)$$

The key point is that θ_c has now become effectively interacting with strength $1+r$. We then rename θ_c as θ'_c due to its new dynamics, thus obtaining Eq. (13).

The dependence on external bias V , the first term in Eq. (19), superficially looks different from that obtained by the first two arguments. However, one can make a time-dependent gauge transformation, similar to that used in obtaining Eq. (10), that moves the bias to the barrier term. The result is exactly Eq. (16), and so the three methods agree.

The strong-coupling effective model is obtained by combining the elements above, resulting in the 0d action

$$S^{\text{eff}} = \frac{1}{\beta} \sum_n |\omega_n| [|\theta_f(\omega_n)|^2 + (1+r)|\theta'_c(\omega_n)|^2] \quad (21a)$$

$$+ A \int d\tau \cos(2\sqrt{\pi}\theta'_c + eV\tau) \cos(2\sqrt{\pi}\theta_f). \quad (21b)$$

In calculating the I - V curve, it will be convenient to have an equivalent Hamiltonian description as well. We first extend the fields to 1d in a way that preserves the 0d action upon integrating out the $x \neq 0$ modes. Then, converting to the Hamiltonian description, we find

$$H^{\text{eff}} = \frac{1}{2} \int_{-\infty}^{\infty} dx \left[(\partial_x \theta_f)^2 + (\partial_x \phi_c)^2 \right] \quad (22a)$$

$$+ (1+r)(\partial_x \theta'_c)^2 + \frac{1}{1+r} (\partial_x \phi'_f)^2 \quad (22b)$$

$$+ A \cos[2\sqrt{\pi}\theta'_c(0) + eVt] \cos[2\sqrt{\pi}\theta_f(0)]. \quad (22c)$$

Note that the modes represented by fields θ_f and ϕ_c are free while those represented by θ'_c and ϕ'_f are interacting.

The coupling between these two sets of modes is given by the barrier term, (21b) or (22c), that describes the deviation from the uniform state characterizing the QCP. Recalling that a bosonic operator of the form $\cos(2\sqrt{\pi}\theta)$ corresponds to backscattering of the underlying fermions, we see that this coupling involves the *simultaneous* backscattering of both sets of modes.

The form of the backscattering term in H^{eff} above is convenient for the calculation of the I - V curve in the next section. We also point out that it is consistent with the form of the backscattering operator in resonant tunneling through a LL at zero bias [43], namely $\cos[2\sqrt{\pi}\theta'(0)]\partial_x\theta'(0)$, where $\theta'(x)$ is the interacting field describing the LL. Note in this regard that both c and f modes are interacting in a LL and related to $\theta'(x)$. To arrive at this form from Eq. (22c), expand about the midpoint of the two barriers and call this point $x=0$. Then from Eq. (15), $\theta'_c \approx \theta'(0)$ and $\theta'_f \approx \partial_x\theta'(0)\ell/2$. In order to expand $\cos[2\sqrt{\pi}\theta'_f(0)]$, note that the fluctuations near the QCP take place about a uniform density such that there is half of a particle in the segment ℓ (the resonance condition). Since $k_F\ell = \pi$ on resonance, the quantity $\tilde{\theta} \equiv \theta' - k_F x/2\sqrt{\pi}$ is small and fluctuating. Using this in θ'_f and then expanding the cosine, one readily finds $\cos[2\sqrt{\pi}\theta'_f] \approx -\pi^{3/2}\partial_x\tilde{\theta}(0)/k_F$. Combining this with $\cos\theta'_c \approx \cos\theta'(0)$, we arrive at the expression above [43] for backscattering from two barriers in a LL.

Returning to our own H^{eff} , note that the bias affects the interacting modes (θ'_c, ϕ'_f) via (21b) or (22c). Physically, this

corresponds to a difference in energy of eV between the forward and backward modes, as can be seen, for instance, by undoing the time-dependent gauge transformation to yield S_μ above and then applying Eq. (18) in reverse. The way the bias enters is, then, entirely consistent with a Landauer-Büttiker approach to weak backscattering.

V. THE I - V CURVE

We first highlight the general features of the I - V curve using a renormalization group (RG) approach, and then turn to a quantitative calculation. The RG scaling equation for the amplitude A of the weak backscattering term Eq. (22c) is

$$\frac{dA}{d \ln D} = \frac{1}{1+r} A, \quad (23)$$

where the energy cutoff D runs from $D_0 = 1$ down to 0—see the supplementary material for an explicit demonstration using standard methods [64]. The scaling dimension of the backscattering operator is then $\Omega \equiv 1 + 1/(1+r)$, showing that the operator is irrelevant and $A \rightarrow 0$ at the QCP. The linear response conductance at zero temperature is thus $G = e^2/h$: perfect transmission for the translationally invariant system defined by Eqs. (22a) and (22b) [35, 42, 43]. From general considerations one expects the low temperature or bias deviation from perfect transmission to be a power law related to this scaling dimension (see, e.g., [43]), namely $|dI/dV - e^2/h| \propto T^{2/(1+r)}$ or $V^{2/(1+r)}$.

To carry the RG treatment further, note that A is thus energy dependent, $A(\epsilon) = A_0 \epsilon^{1/(1+r)}$ where A_0 is a constant. This power-law scaling is cut off below T , making A temperature dependent as well, $A(\epsilon, T)$. The differential conductance $G(V, T) = dI/dV$ can be obtained approximately by integrating the spectral function of the transmission probability $T(\epsilon, T) = 1 - R(\epsilon, T)$ over ϵ via Eq. (23) with $R \propto A^2$. Note that a more accurate but technically complex RG treatment would involve computing $R(\epsilon, T, V)$ out of equilibrium at a finite bias V . We make the approximation $R \approx R(\epsilon, T, V=0)$ here. The approximate non-linear current therefore reads,

$$I(V, T) \approx \frac{e}{h} \int_{-D_0}^{D_0} d\epsilon [1 - R(\epsilon, T)] [f_R(\epsilon) - f_L(\epsilon)], \quad (24)$$

where $f_{L/R}(\epsilon)$ refers to the Fermi-Dirac distribution. The normalized reflection probability $R(V, T)/R(0, T)$ from (24) exhibits a crossover from power-law behavior in V/T for $V/T > 1$,

$$R(V, T)/R(0, T) \approx (V/T)^{2/(1+r)}, \quad (25)$$

to 1 for $V/T \rightarrow 0$, as expected from the general considerations.

Given these basic features of the I - V curve, we now turn to an explicit calculation: we find the correction to the perfect QCP transmission to leading order in A by applying Fermi's golden rule to find the backscattering rate, Γ . The backscattering matrix element needed in Fermi's golden rule is [39]

$$\langle f | H_T | i \rangle = A \langle R_1^f | \cos[2\sqrt{\pi}\theta'_c(0)] | R_1^i \rangle \times \langle R_2^f | \cos[2\sqrt{\pi}\theta'_f(0)] | R_2^i \rangle, \quad (26)$$

where $|R_1\rangle$ and $|R_2\rangle$ represent the states of θ'_c and θ'_f , respectively, and i and f label the initial and final states. Recall that in time-dependent perturbation theory, an explicit oscillatory time dependence such as in Eq. (22c) factors out and enters the energy conservation constraint. The rate is, then, given by

$$\begin{aligned} \Gamma(V, T) = & A^2 \frac{2\pi}{\hbar} \sum_{R_1^i R_1^f} \sum_{R_2^i R_2^f} \\ & \times |\langle R_1^f | \cos[2\sqrt{\pi}\theta'_c(0)] | R_1^i \rangle|^2 P_\beta(R_1^i) \\ & \times |\langle R_2^f | \cos[2\sqrt{\pi}\theta'_f(0)] | R_2^i \rangle|^2 P_\beta(R_2^i) \\ & \times \delta(E_{R_1^i} + E_{R_2^i} + eV - E_{R_1^f} - E_{R_2^f}), \end{aligned} \quad (27)$$

where $P_\beta(R_{1,2}^i) = \langle R_{1,2}^i | \rho_\beta | R_{1,2}^i \rangle$ refers to the density matrices of the fields and the subscript β is a reminder of the thermal effect.

To evaluate the rate, first rewrite the δ -function as an integral over time of an exponential. Then, notice that the factors $\exp(iE_{i,f}t/\hbar)$ can be produced by acting on the initial or final state with $\exp(iHt/\hbar)$. Thus, changing to the Heisenberg picture for the fields and dropping the argument $x = 0$ for clarity, we find

$$\begin{aligned} \Gamma(V, T) = & \frac{A^2}{\hbar^2} \int_{-\infty}^{\infty} dt \sum_{R_1^i R_1^f} \langle R_1^i | \cos[2\sqrt{\pi}\theta'_c(t)] | R_1^f \rangle \langle R_1^f | \cos[2\sqrt{\pi}\theta'_c(t=0)] | R_1^i \rangle P_\beta(R_1^i) \\ & \times \sum_{R_2^i R_2^f} \langle R_2^i | \cos[2\sqrt{\pi}\theta'_f(t)] | R_2^f \rangle \langle R_2^f | \cos[2\sqrt{\pi}\theta'_f(t=0)] | R_2^i \rangle P_\beta(R_2^i) e^{ieVt/\hbar} \\ = & \frac{A^2}{\hbar^2} \int_{-\infty}^{\infty} dt e^{ieVt/\hbar} \langle \cos[2\sqrt{\pi}\theta'_c(t)] \cos[2\sqrt{\pi}\theta'_c(0)] \rangle \langle \cos[2\sqrt{\pi}\theta'_f(t)] \cos[2\sqrt{\pi}\theta'_f(0)] \rangle. \end{aligned} \quad (28)$$

Evaluation of the bosonic correlation function is standard, see for example Refs. [51, 56]. In terms of the scaling dimension

$\Omega = 1 + 1/(1+r)$ of the backscattering operator, the result for the rate is

$$\begin{aligned}\Gamma(V, T) &= \frac{A^2}{4\hbar^2} \int_{-\infty}^{\infty} dt e^{ieVt/\hbar} \exp \left[-2\Omega \ln \sinh \left(\frac{\pi k_B T |t|}{\hbar} \right) + 2\Omega \ln \frac{\pi k_B T}{\hbar \omega_R} - \Omega i \pi \text{Sign}(t) - 2\Omega \gamma \right] \\ &= \frac{A^2}{4\hbar^2} \frac{\pi}{\Gamma(2\Omega)} \left(\frac{2\pi k_B T}{\hbar \omega_R} \right)^{2\Omega-1} \frac{1}{\omega_R} \exp \left(\frac{eV}{2k_B T} \right) \left| \Gamma \left(\Omega + i \frac{eV}{2\pi k_B T} \right) \right|^2,\end{aligned}\quad (29)$$

where ω_R is the energy cutoff of the bosonic bath and γ is Euler's constant. Physically, as this rate involves gain of energy, it corresponds to backscattering from the right-moving to left-moving channel [using the convention of Eqs. (3) and (18)]. The net current is related to the difference of this rate and that in the opposite sense, namely $\Gamma(-V, T)$. Since the energy associated with the bias in each backscattering event is eV , we conclude that the charge carried by each quasi-particle is e . Consequently, the backscattering-related current is $\Delta I(V, T) = e[\Gamma(V, T) - \Gamma(-V, T)]$. Adding this to the perfect transmission when $A = 0$, we arrive at our final result for the I - V curve

$$I(V, T) = \frac{e^2}{h} V \left\{ 1 - \frac{A^2 \pi^2}{\hbar^2 \omega_R^2} \frac{1}{\Gamma(\frac{2}{1+r} + 2)} \left(\frac{2\pi k_B T}{\hbar \omega_R} \right)^{\frac{2}{1+r}} \left| \frac{\Gamma \left(\frac{1}{1+r} + 1 + i \frac{eV}{2\pi k_B T} \right)}{\Gamma \left(1 + i \frac{eV}{2\pi k_B T} \right)} \right|^2 \right\}.\quad (30)$$

This is the main theoretical result of this paper: the nonlinear I - V curve to leading order in the backscattering amplitude A near the strong-coupling QCP. Flow to this QCP occurs by tuning the system (described by the original microscopic Hamiltonian in Sec. II) to be on resonance and to have symmetric source and drain barriers. For a plot of this curve see the comparison with experiment below (Sec. VII). Note that for large bias, the expected power law is obtained, $|dI/dV - e^2/h| \propto V^{2/(1+r)}$.

VI. INTERPRETATION VIA DYNAMICAL COULOMB BLOCKADE

To enhance the physical understanding of this result, we rewrite our strong coupling effective system as a fermionic problem and thereby make a direct connection to dynamical Coulomb blockade (DCB) theory. In order to use non-interacting fermions, we choose to refermionize the non-interacting bosonic fields (θ_f, ϕ_c) in Eq. (22), using the bosonization relation Eq. (6) where α now denotes this pair. It is also convenient to move the bias out of the barrier term by undoing the time-dependent gauge transformation. The coupling term Eq. (22c) is, then, replaced by the two terms

$$\begin{aligned}H_T &= \pi a_0 A \cos [2\sqrt{\pi} \theta'_c(0)] [\psi_L^\dagger(0) \psi_R(0) + \text{h.c.}] \\ H_\mu &= -eV \theta'_c(0) / \sqrt{4\pi}.\end{aligned}\quad (31)$$

The fact that the bias couples to the interacting field θ'_c is a serious complication. However, note that we will calculate the I - V curve only to leading order in A , via Fermi's golden rule as in the last section. In the expression for the rate, the bias appears only in the energy-conservation δ -function as the particle gains (or loses) energy eV when it backscatters. Note that the excitations of θ'_c and θ_f are tightly linked in the single term in Eq. (22c), leading to a single connection between a

given $|i\rangle$ and its $|f\rangle$. Thus, whether the energy eV comes from coupling to the interacting or non-interacting field cannot be distinguished at this order. We can, then, calculate the I - V curve using the bias term

$$H'_\mu = -eV \theta'_f(0) / \sqrt{4\pi}.\quad (32)$$

Refermionizing this term using relations analogous to those in Eq. (18), we arrive at the auxiliary model

$$\begin{aligned}H' &= \frac{1}{2} \int_{-\infty}^{\infty} dx [\psi_R^\dagger(x) \partial_x \psi_R(x) - \psi_L^\dagger(x) \partial_x \psi_L(x)] \\ &+ \frac{1}{2} \int_{-\infty}^{\infty} dx \left[(1+r) (\partial_x \theta'_c)^2 + \frac{1}{1+r} (\partial_x \phi'_f)^2 \right] \\ &+ \pi a_0 A \cos [2\sqrt{\pi} \theta'_c(0)] \{ \psi_L^\dagger(0) \psi_R(0) + \text{h.c.} \} \\ &+ \frac{eV}{2} \left[\int_{-\infty}^0 dx \psi_R^\dagger(x) \psi_R(x) - \int_0^{\infty} dx \psi_L^\dagger(x) \psi_L(x) \right].\end{aligned}\quad (33)$$

Each line of (S9) can be interpreted physically: the first line is right- and left- moving non-interacting fermions, second line is an interacting bosonic environment, third line shows that backscattering of the fermions excites the environment, and fourth line accounts for the voltage bias between the right- and left- moving fermions.

We thus recognize the form for tunneling of non-interacting particles through a barrier in the presence of an environment, albeit with a strange barrier and strange environment. Tunneling through the barrier consists of backscattering between two chiral fermion modes, and the environment θ'_c involves a nonlinear combination of the original electrons and environment [the rotation Eq. (11) applies to quantities in the exponent]. Nevertheless, the standard techniques of DCB theory [51–53] can be applied to obtain the nonlinear I - V curve to second order in A . The result [39, 64, 65] is the same as in the last section, Eq. (30), with the coefficient of the correction $(A\pi/\hbar\omega_R)^2$ replaced by $(h/e^2)/R_T$, where R_T is the

tunneling resistance of the effective barrier in the absence of dissipation.

The equivalence of these two coefficients is shown by considering the auxiliary model (S9). Denote the backscattering amplitude of the fermions by $t_{k,q}$, where k and q label the initial and final fermionic particle states, $H_T = \sum_{k,q} t_{k,q} c_{L,k}^\dagger c_{R,q}$. The standard result for the conductance of a tunneling barrier when the amplitude is momentum independent is $1/R_T = (e^2/h) |\bar{t}|^2 [\Xi N(0)]^2$, where $\Xi N(0)$ is the number of states per unit energy and \bar{t} is the average matrix element. In our case, the number of states is the size of the system L divided by the bosonization cutoff a_0 , and the maximum energy for a particle excitation is $\hbar\omega_R$, the cutoff for the bosonic modes ($-\hbar\omega_R$ for a hole excitation). The amplitude \bar{t} follows from Eq. (S9) noting that a factor of $1/L$ is introduced in the conversion from continuous x to discrete k . Putting these elements together one finds

$$\frac{1}{R_T} = \frac{e^2}{h} \left(\frac{\pi a_0 A}{L} \right)^2 \left(\frac{L/a_0}{\hbar\omega_R} \right)^2 = \frac{e^2}{h} \left(\frac{\pi A}{\hbar\omega_R} \right)^2. \quad (34)$$

Thus the I - V curve that results from a DCB theory treatment of the auxiliary strong-coupling model (S9) and that found from the true effective bosonic description (22) are identical.

This allows then the physically intuitive interpretation of the I - V curve Eq. (30) as tunneling of non-interacting fermions (from left-movers to right-movers) in the presence of an environment, and we will refer to (30) as the result of DCB theory.

VII. COMPARISON TO EXPERIMENT

Experiments were performed on quantum dots fabricated from carbon nanotubes contacted by Cr/Au electrodes. The electrodes were further connected to the bonding pads by Cr resistors that provided dissipation. In Fig. 2 we show data from two samples with $r = 0.5$ and $r = 0.75$. The conductance G is measured in units of e^2/h and rescaled such that at a given temperature $1 - G(V)$ is divided by $1 - G(V=0)$.

The purpose of Fig. 2 is to compare the experimental data to the theoretical expressions. Both the full non-linear result (30) and the approximate RG-based result (24) are shown, and both capture the overall experimental behavior remarkably well. Note that there are no free parameters in the theory—this is not a fit. Indeed, the value of r is determined in an independent equilibrium measurement of $G(T)$ off resonance [35], after which $1 - G$ is shown to scale as $T^{2/(1+r)}$ [36].

It is important to realize that, unlike measurements that use a weakly coupled contact to probe the equilibrium density of states at finite bias (for example [66–69]), here the two biased contacts remain equally coupled to the quantum dot, creating genuinely non-equilibrium conditions [18, 70].

Comparing closely the experimental and DCB results, we see two striking features of the theory: first, it captures the *crossover regime* $eV \sim kT$ very accurately, and, second, it yields the correct *prefactor* of the universal $\propto V^{2/(1+r)}$ dependence at high bias [71]. (For other ways of plotting the

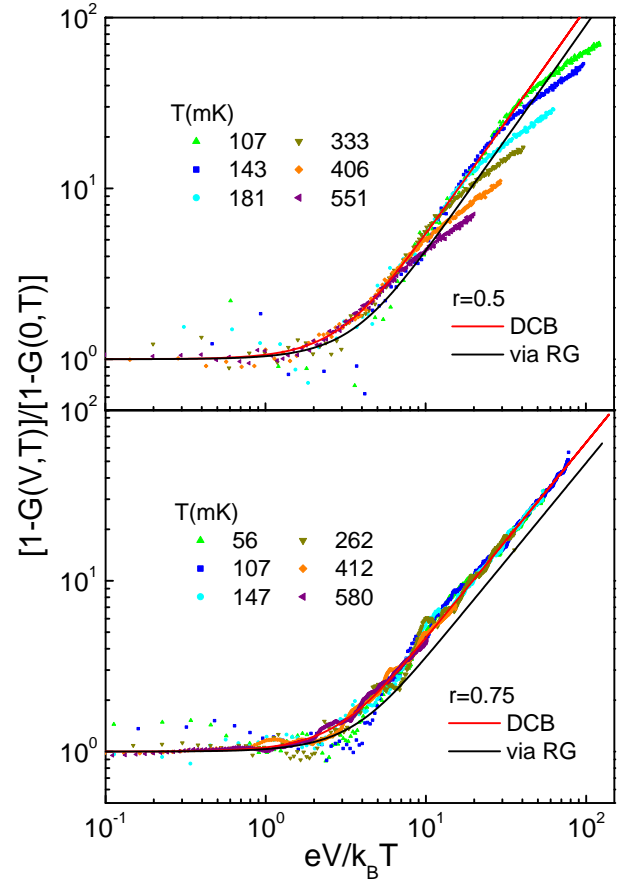


FIG. 2. Deviation from perfect conductance $1 - G(V, T)$, scaled by $1 - G(V = 0, T)$, as a function of $eV/k_B T$ for $r = 0.5$ (top) and $r = 0.75$ (bottom). Here $G(V, T)$ is the differential conductance $G = (h/e^2) dI/dV$. The symbols are the experimental results at the color-coded temperatures. The red and black lines are the results of the DCB and RG theories [Eqs. (30) and (24)], respectively, in which there are no free parameters. Note the excellent agreement between the DCB result and the data in both the crossover and power-law regimes. At larger V/T , non-universal effects begin to set in due to $1 - G(V, T)$ becoming non-negligible compared to 1.

$r = 0.5$ data, see the supplemental material [64].) The difference between the DCB result and the RG approximation is, on the other hand, quite noticeable: in the universal regime, the DCB theory falls on top of the data, while the RG result is consistently too small. *The excellent agreement between the DCB theory and experiment in a wide range of $eV/k_B T$ is a striking confirmation of our far-from-equilibrium calculation.*

At high enough $eV/k_B T$, the experimental curves deviate from the theoretical prediction (Fig. 2, top). The reason for this discrepancy is that $1 - G$ is no longer small, and so higher order scattering terms not included in our effective strong-coupling model or Fermi's golden rule analysis cannot be neglected. The range of applicability of our analytical results is pushed to higher and higher $eV/k_B T$ as the temperature is lowered.

VIII. CONCLUSIONS

We have carried out an analytic calculation of a far-from-equilibrium I - V curve at a strong-coupling QCP, and then presented experimental results enabling a detailed theory-experiment comparison. The calculation is made possible through an effective bosonic description at strong-coupling. The agreement with the experimental results throughout the crossover and asymptotic regimes, as shown in Fig. 2, is excellent.

A simple physical interpretation is possible because only one of the charge modes in the system couples to the EM environment, leaving the mode corresponding to fluctuations of the total charge in the dot free. This feature is not present, for instance, in the related problem of resonant tunneling in a Luttinger liquid. It allows us to find the I - V curve, alternatively, from the problem of tunneling between left- and right-moving non-interacting fermions in the presence of a modified environment. The solution to that problem from dynamical Coulomb blockade theory yields an explicit expression for

the nonlinear I - V curve which is identical to that from the bosonic description.

To our knowledge, this is the first calculation or measurement of the nonequilibrium nonlinear I - V curve at a QCP. A remarkable aspect of this system is that it is fully accessible to both theory and experiment, allowing for a detailed comparison between the two. As non-equilibrium results at a QCP are exceedingly rare, this provides a valuable bench mark and test case for future studies of non-equilibrium steady states.

ACKNOWLEDGMENTS

We thank E. Novais for helpful discussions. The work in Taiwan (CHC and CYL) was supported by the NSC grants No.98-2918-I-009-06 and No.98-2112-M-009-010-MY3, the MOE-ATU program, and the NCTS of Taiwan, R.O.C. The work in the U.S.A. was supported by the U.S. DOE Office of Science, Division of Materials Sciences and Engineering, under Grants Nos. DE-SC0005237 (GZ and HUB, theory), DE-SC0002765 (CTK, HM, and GF, experiment), and DE-FG02-02ER15354 (AIS, experiment).

-
- [1] Lincoln D. Carr, *Understanding Quantum Phase Transitions* (CRC Press, Boca Raton, Florida, 2011).
 - [2] Subir Sachdev, *Quantum Phase Transitions*, 2nd ed. (Cambridge University Press, Cambridge, 2011).
 - [3] M. Vojta, “Impurity quantum phase transitions,” *Philos. Mag.* **86**, 1807–1846 (2006).
 - [4] L. Amico, R. Fazio, A. Osterloh, and V. Vedral, “Entanglement in many-body systems,” *Rev. Mod. Phys.* **80**, 517–576 (2008).
 - [5] A. Polkovnikov, K. Sengupta, A. Silva, and M. Vengalattore, “Colloquium: Nonequilibrium dynamics of closed interacting quantum systems,” *Rev. Mod. Phys.* **83**, 863–883 (2011).
 - [6] H. Aoki, N. Tsuji, M. Eckstein, M. Kollar, T. Oka, and P. Werner, “Nonequilibrium dynamical mean-field theory and its applications,” *Rev. Mod. Phys.* **86**, 779–837 (2014).
 - [7] J. Eisert, M. Friesdorf, and C. Gogolin, “Quantum many-body systems out of equilibrium,” *Nat. Phys.* **11**, 124–130 (2015).
 - [8] A. M. Chang, “Chiral Luttinger liquids at the fractional quantum Hall edge,” *Rev. Mod. Phys.* **75**, 1449–1505 (2003).
 - [9] M. Grobis, I. G. Rau, R. M. Potok, and D. Goldhaber-Gordon, “Kondo effect in mesoscopic quantum dots,” in *Handbook of Magnetism and Advanced Magnetic Materials*, Vol. 5, edited by H. Kronmüller and S. Parkin (Wiley, New York, 2007) pp. 2703–2724, and arXiv:cond-mat/0611480.
 - [10] A. M. Chang and J. C. Chen, “The Kondo effect in coupled-quantum dots,” *Rep. Prog. Phys.* **72**, 096501 (2009).
 - [11] A. P. Micolich, “What lurks below the last plateau: Experimental studies of the 0.7 conductance anomaly in one-dimensional systems,” *J. Phys. Cond. Matt.* **23**, 443201 (2011).
 - [12] A. Martín-Rodero and A. Levy-Yeyati, “Josephson and Andreev transport through quantum dots,” *Adv. Phys.* **60**, 899–958 (2011).
 - [13] I. G. Rau, S. Amasha, Y. Oreg, and D. Goldhaber-Gordon, “Quantum phase transitions in quantum dots,” in *Understanding Quantum Phase Transitions*, edited by L. D. Carr (CRC Press, Boca Raton, 2011) pp. 341–367.
 - [14] A. V. Kretinin, H. Shtrikman, D. Goldhaber-Gordon, M. Hanl, A. Weichselbaum, J. von Delft, T. Costi, and D. Mahalu, “Spin- $\frac{1}{2}$ kondo effect in an inas nanowire quantum dot: Unitary limit, conductance scaling, and zeeman splitting,” *Phys. Rev. B* **84**, 245316 (2011).
 - [15] R. Maurand, T. Meng, E. Bonet, S. Florens, L. Marty, and W. Wernsdorfer, “First-order 0 - π quantum phase transition in the Kondo regime of a superconducting carbon-nanotube quantum dot,” *Phys. Rev. X* **2**, 011009 (2012).
 - [16] S. Jezouin, M. Albert, F. D. Parmentier, A. Anthore, U. Gennser, A. Cavanna, I. Safi, and F. Pierre, “Tomonaga-Luttinger physics in electronic quantum circuits,” *Nat. Commun.* **4**, 1802 (2013).
 - [17] M. Ferrier, T. Arakawa, T. Hata, R. Fujiwara, R. Delagrangé, R. Weil, R. Deblock, R. Sakano, A. Oguri, and K. Kobayashi, “Universality of non-equilibrium fluctuations in strongly correlated quantum liquids,” *Nat. Phys.* **12**, 230–235 (2016).
 - [18] Y. Meir and N. S. Wingreen, “Landauer formula for the current through an interacting electron region,” *Phys. Rev. Lett.* **68**, 2512–2515 (1992).
 - [19] P. Fendley, A. W. W. Ludwig, and H. Saleur, “Exact nonequilibrium transport through point contacts in quantum wires and fractional quantum Hall devices,” *Phys. Rev. B* **52**, 8934–8950 (1995).
 - [20] A. Schiller and S. Hershfield, “Toulouse limit for the nonequilibrium Kondo impurity: Currents, noise spectra, and magnetic properties,” *Phys. Rev. B* **58**, 14978 (1998); K. Majumdar, A. Schiller, and S. Hershfield, “Nonequilibrium Kondo impurity: Perturbation about an exactly solvable point,” *Phys. Rev. B* **57**, 2991–2999 (1998).
 - [21] A. Rosch, J. Paaske, J. Kroha, and P. Wölfle, “Nonequilibrium transport through a Kondo dot in a magnetic field: Perturbation theory and poor man’s scaling,” *Phys. Rev. Lett.* **90**, 076804 (2003).

- [22] F. Heidrich-Meisner, A. E. Feiguin, and E. Dagotto, “Real-time simulations of nonequilibrium transport in the single-impurity Anderson model,” *Phys. Rev. B* **79**, 235336 (2009).
- [23] C.-H. Chung, K. Le Hur, M. Vojta, and P. Wölfle, “Nonequilibrium transport at a dissipative quantum phase transition,” *Phys. Rev. Lett.* **102**, 216803 (2009); C.-H. Chung, K. Le Hur, G. Finkelstein, M. Vojta, and P. Wölfle, “Nonequilibrium quantum transport through a dissipative resonant level,” *Phys. Rev. B* **87**, 245310 (2013).
- [24] I. Safi and P. Joyez, “Time-dependent theory of nonlinear response and current fluctuations,” *Phys. Rev. B* **84**, 205129 (2011).
- [25] V. Koerting, B. M. Andersen, K. Flensberg, and J. Paaske, “Nonequilibrium transport via spin-induced subgap states in superconductor/quantum dot/normal metal cotunnel junctions,” *Phys. Rev. B* **82**, 245108 (2010).
- [26] M. Pletyukhov and H. Schoeller, “Nonequilibrium Kondo model: Crossover from weak to strong coupling,” *Phys. Rev. Lett.* **108**, 260601 (2012).
- [27] G. Cohen, E. Gull, D. R. Reichman, and A. J. Millis, “Green’s Functions from Real-Time Bold-Line Monte Carlo Calculations: Spectral Properties of the Nonequilibrium Anderson Impurity Model,” *Phys. Rev. Lett.* **112**, 146802 (2014).
- [28] R. Härtle and A. J. Millis, “Formation of nonequilibrium steady states in interacting double quantum dots: When coherences dominate the charge distribution,” *Phys. Rev. B* **90**, 245426 (2014).
- [29] A. Dorda, M. Ganahl, H. G. Evertz, W. von der Linden, and E. Arrigoni, “Auxiliary master equation approach within matrix product states: Spectral properties of the nonequilibrium Anderson impurity model,” *Phys. Rev. B* **92**, 125145 (2015).
- [30] C. Altimiras, F. Portier, and P. Joyez, “Interacting electrodynamics of short coherent conductors in quantum circuits,” *Phys. Rev. X* **6**, 031002 (2016).
- [31] E. Sela and I. Affleck, “Nonequilibrium transport through double quantum dots: Exact results near a quantum critical point,” *Phys. Rev. Lett.* **102**, 047201 (2009).
- [32] E. Sela and I. Affleck, “Nonequilibrium critical behavior for electron tunneling through quantum dots in an Aharonov-Bohm circuit,” *Phys. Rev. B* **79**, 125110 (2009).
- [33] A. K. Mitchell, L. A. Landau, L. Fritz, and E. Sela, “Universality and scaling in a charge two-channel Kondo device,” *Phys. Rev. Lett.* **116**, 157202 (2016).
- [34] Yu. Bomze, H. Mebrahtu, I. Borzenets, A. Makarovski, and G. Finkelstein, “Resonant tunneling in a dissipative environment,” *Phys. Rev. B* **79**, 241402 (2009).
- [35] H. T. Mebrahtu, I. V. Borzenets, Dong E. Liu, Huaixiu Zheng, Yu. V. Bomze, A. I. Smirnov, H. U. Baranger, and G. Finkelstein, “Quantum phase transition in a resonant level coupled to interacting leads,” *Nature* **488**, 61–64 (2012).
- [36] H. T. Mebrahtu, I. V. Borzenets, H. Zheng, Yu. V. Bomze, A. I. Smirnov, S. Florens, H. U. Baranger, and G. Finkelstein, “Observation of Majorana quantum critical behavior in a resonant level coupled to a dissipative environment,” *Nat. Phys.* **9**, 732–737 (2013), arXiv:1212.3857.
- [37] K. A. Matveev and L. I. Glazman, “Coulomb blockade of tunneling into a quasi-one-dimensional wire,” *Phys. Rev. Lett.* **70**, 990–993 (1993).
- [38] Karsten Flensberg, “Capacitance and conductance of mesoscopic systems connected by quantum point contacts,” *Phys. Rev. B* **48**, 11156–11166 (1993).
- [39] M. Sassetti and U. Weiss, “Transport of 1d interacting electrons through barriers and effective tunnelling density of states,” *EPL (Europhysics Letters)* **27**, 311 (1994).
- [40] I. Safi and H. Saleur, “One-channel conductor in an Ohmic environment: Mapping to a Tomonaga-Luttinger liquid and full counting statistics,” *Phys. Rev. Lett.* **93**, 126602 (2004).
- [41] K. Le Hur and Mei-Rong Li, “Unification of electromagnetic noise and Luttinger liquid via a quantum dot,” *Phys. Rev. B* **72**, 073305 (2005).
- [42] C. L. Kane and M. P. A. Fisher, “Transmission through barriers and resonant tunneling in an interacting one-dimensional electron gas,” *Phys. Rev. B* **46**, 15233–15262 (1992); “Resonant tunneling in an interacting one-dimensional electron gas,” *Phys. Rev. B* **46**, 7268–7271(R) (1992).
- [43] S. Eggert and I. Affleck, “Magnetic impurities in half-integer-spin Heisenberg antiferromagnetic chains,” *Phys. Rev. B* **46**, 10866–10883 (1992).
- [44] A. Furusaki and N. Nagaosa, “Resonant tunneling in a Luttinger liquid,” *Phys. Rev. B* **47**, 3827–3831 (1993).
- [45] A. Furusaki, “Resonant tunneling through a quantum dot weakly coupled to quantum wires or quantum Hall edge states,” *Phys. Rev. B* **57**, 7141–7148 (1998).
- [46] Yu. V. Nazarov and L. I. Glazman, “Resonant tunneling of interacting electrons in a one-dimensional wire,” *Phys. Rev. Lett.* **91**, 126804 (2003).
- [47] D. G. Polyakov and I. V. Gornyi, “Transport of interacting electrons through a double barrier in quantum wires,” *Phys. Rev. B* **68**, 035421 (2003).
- [48] A. Komnik and A. O. Gogolin, “Resonant tunneling between Luttinger liquids: A solvable case,” *Phys. Rev. Lett.* **90**, 246403 (2003).
- [49] V. Meden, T. Enss, S. Andergassen, W. Metzner, and K. Schönhammer, “Correlation effects on resonant tunneling in one-dimensional quantum wires,” *Phys. Rev. B* **71**, 041302 (2005).
- [50] M. Goldstein and R. Berkovits, “Duality between different geometries of a resonant level in a Luttinger liquid,” *Phys. Rev. Lett.* **104**, 106403 (2010).
- [51] G.-L. Ingold and Yu. V. Nazarov, “Charge tunneling rates in ultrasmall junctions,” in *Single Charge Tunneling: Coulomb Blockade Phenomena in Nanostructures*, edited by H. Grabert and M. H. Devoret (Plenum, New York, 1992) pp. 21–107, and arXiv:cond-mat/0508728.
- [52] Yu. V. Nazarov and Y. M. Blanter, *Quantum Transport: Introduction to Nanoscience* (Cambridge University Press, Cambridge, 2009).
- [53] M. H. Devoret, D. Esteve, and C. Urbina, “Single electron phenomena in metallic nanostructures,” in *Mesoscopic Quantum Physics: Les Houches Session LXI*, edited by E. Akkermans, G. Montambaux, Pichard J.-L., and J. Zinn-Justin (Elsevier, Amsterdam, 1995) pp. 605–658.
- [54] M. H. Devoret, “Quantum fluctuations in electrical circuits,” in *Quantum Fluctuations: Les Houches Session LXIII*, edited by S. Reynaud, E. Giacobino, and J. Zinn-Justin (Elsevier, Amsterdam, 1997) p. 351.
- [55] Dong E. Liu, Huaixiu Zheng, G. Finkelstein, and H. U. Baranger, “Tunable quantum phase transitions in a resonant level coupled to two dissipative baths,” *Phys. Rev. B* **89**, 085116 (2014).
- [56] Thierry Giamarchi, *Quantum Physics in One Dimension* (Oxford University Press, New York, 2004).
- [57] Ulrich Weiss, *Quantum Dissipative Systems*, 4th ed. (World Scientific, Singapore, 2012).
- [58] J. Honer and U. Weiss, “Nonlinear conductance and noise in boundary sine-gordon and related models,” *Chemical Physics* **375**, 265 – 275 (2010), in Stochastic processes in Physics and Chemistry (in honor of Peter Hänggi).

- [59] The effective action of our problem maps to that of 1d quantum Brownian motion [72]. Ref. [57] discusses the duality between weak and strong coupling in that case (Section 26, “Duality Symmetry”).
- [60] At the QCP, certain degrees of freedom associated with the dot become decoupled and contribute a boundary entropy. The best known example is the $\ln(\sqrt{2})$ entropy at the Emery-Kivelson point due to the decoupled Majorana fermion. In our case, the boundary entropy can be calculated from conformal field theory to be $\ln(\sqrt{1+r})$ [73, 74]. These decoupled degrees of freedom do not affect the I - V curve.
- [61] Y. Imry and R. Landauer, “Conductance viewed as transmission,” *Rev. Mod. Phys.* **71**, S306–S312 (1999).
- [62] M. Büttiker, “Four-terminal phase-coherent conductance,” *Phys. Rev. Lett.* **57**, 1761–1764 (1986).
- [63] Thomas Ihn, *Semiconductor Nanostructures* (Oxford University Press, Oxford, 2010).
- [64] In the Supplemental Material, we address (i) the derivation of the RG equation (23) given in the main text, (ii) the calculation of the final expression for the I - V curve in Eq. (30) using DCB theory, and (iii) the plotting of the $r=0.5$ data on different scales.
- [65] W. Zheng, J. R. Friedman, D. V. Averin, S. Y. Han, and J. E. Lukens, “Observation of strong Coulomb blockade in resistively isolated tunnel junctions,” *Sol. State Comm.* **108**, 839–843 (1998).
- [66] R. Leturcq, L. Schmid, K. Ensslin, Y. Meir, D. C. Driscoll, and A. C. Gossard, “Probing the Kondo density of states in a three-terminal quantum ring,” *Phys. Rev. Lett.* **95**, 126603 (2005).
- [67] A. Makarovski, J. Liu, and G. Finkelstein, “Evolution of transport regimes in carbon nanotube quantum dots,” *Phys. Rev. Lett.* **99**, 066801 (2007).
- [68] R. M. Potok, I. G. Rau, H. Shtrikman, Y. Oreg, and D. Goldhaber-Gordon, “Observation of the two-channel Kondo effect,” *Nature* **446**, 167–171 (2007).
- [69] A. J. Keller, L. Peeters, C. P. Moca, I. Weymann, D. Mahalu, V. Umansky, G. Zarand, and D. Goldhaber-Gordon, “Universal Fermi liquid crossover and quantum criticality in a mesoscopic system,” *Nature* **526**, 237–240 (2015).
- [70] M. Pustilnik, L. Borda, L. I. Glazman, and J. von Delft, “Quantum phase transition in a two-channel-Kondo quantum dot device,” *Phys. Rev. B* **69**, 115316 (2004).
- [71] The absolute magnitude of the current in the power-law scaling regime is a key prediction of weak-coupling DCB theory. Here, because of the unknown amplitude A in the effective strong-coupling model Eq. (22) or (S9), we do not have such a prediction. However, for the normalized quantity plotted, DCB theory does give a definite value of the prefactor because it is fixed by the way the theory transitions from the cross-over to the asymptotic regime.
- [72] Hangmo Yi and C. L. Kane, “Quantum Brownian motion in a periodic potential and the multichannel Kondo problem,” *Phys. Rev. B* **57**, R5579–R5582 (1998).
- [73] E. Wong and I. Affleck, “Tunneling in quantum wires: A boundary conformal field theory approach,” *Nucl. Phys. B* **417**, 403–438 (1994).
- [74] H. Zheng, S. Florens, and H. U. Baranger, “Transport signatures of Majorana quantum criticality realized by dissipative resonant tunneling,” *Phys. Rev. B* **89**, 235135 (2014).
-

Supplemental Material for “Universal Nonlinear I-V Curve at an Interacting Impurity Quantum Critical Point”

Gu Zhang, Chung-Hou Chung, Chung-Ting Ke, Chao-Yun Lin, Henok Mebrahtu, Alex I. Smirnov, Gleb Finkelstein, and Harold U. Baranger
(Dated: August 02, 2017)

In this Supplemental Material, we provide details on three topics in the main text: (i) the derivation of the RG equation (23) given in the main text, (ii) the calculation of the final expression for the I - V curve in Eq. (30) of the main text using DCB theory, and (iii) the plotting of the $r=0.5$ data on axes other than the log-log shown in Fig. 2 of the main text.

I. RENORMALIZATION GROUP EQUATION TO TREE LEVEL

In this section, we provide a detailed derivation of Eq. (23) in the main text using standard methods. Basic techniques in this section come from the book “Condensed Matter Field Theory” [S1].

We start with the effective zero-dimensional action Eq. (21) in the main text with $V=0$ (i.e. in equilibrium)

$$\begin{aligned} S^{\text{eff}} &= S_0^{\text{eff}} + S_T \\ &= \frac{1}{\beta} \sum_{\omega_n} |\omega_n| [|\theta_f(\omega_n)|^2 + (1+r)|\theta'_c(\omega_n)|^2] + A \int d\tau \cos [2\sqrt{\pi}\theta'_c(\tau)] \cos [2\sqrt{\pi}\theta_f(\tau)] \\ &= \int_{|\omega|<\Lambda} \frac{d\omega}{2\pi} [|\theta_f(\omega)|^2|\omega| + (1+r)|\theta'_c(\omega)|^2|\omega|] + A \int d\tau \cos [2\sqrt{\pi}\theta'_c(\tau)] \cos [2\sqrt{\pi}\theta_f(\tau)], \end{aligned} \quad (\text{S1})$$

where Λ is the energy cutoff and the substitution $\sum_{\omega_n} \rightarrow \int d\omega \frac{\beta}{2\pi}$ is used to write the free action into its integral form. As typical for RG, we decrease the cutoff from Λ to $\Lambda - d\Lambda$ and divide the field into the fast and slow modes

$$\begin{aligned} \theta(\tau) &= \frac{1}{\beta} \int \frac{d\omega}{2\pi} e^{-i\omega\tau} \theta(\omega) \\ &= \frac{1}{\beta} \int_{|\omega|<\Lambda-d\Lambda} \frac{d\omega}{2\pi} e^{-i\omega\tau} \theta(\omega) + \frac{1}{\beta} \int_{\Lambda-d\Lambda<|\omega|<\Lambda} \frac{d\omega}{2\pi} e^{-i\omega\tau} \theta(\omega) \\ &\equiv \theta_{<}(\tau) + \theta_{>}(\tau), \end{aligned} \quad (\text{S2})$$

where $>$ and $<$ represent the fast and slow modes, respectively. Based on these definitions, the action is divided into three parts: $S^{\text{eff}} = S_{<}^{\text{eff}} + S_{>}^{\text{eff}} + S_I^{\text{eff}}$ where $>$, $<$, and I represent the fast mode, the slow mode, and the interaction between them, respectively, with

$$\begin{aligned} S_{<}^{\text{eff}} &= \int_{|\omega|<\Lambda-d\Lambda} \frac{d\omega}{2\pi} [|\theta_f(\omega)|^2|\omega| + (1+r)|\theta'_c(\omega)|^2|\omega|] \\ S_{>}^{\text{eff}} &= \int_{\Lambda-d\Lambda<|\omega|<\Lambda} \frac{d\omega}{2\pi} [|\theta_f(\omega)|^2|\omega| + (1+r)|\theta'_c(\omega)|^2|\omega|] \\ S_I^{\text{eff}} &= A \int d\tau \cos \{2\sqrt{\pi} [\theta'_{c<}(\tau) + \theta'_{c>}(\tau)]\} \cos \{2\sqrt{\pi} [\theta_{f<}(\tau) + \theta_{f>}(\tau)]\}. \end{aligned} \quad (\text{S3})$$

Notice that the $>$ and $<$ parts come from the free quadratic action while the I part comes from the backscattering term.

In the RG method, parameters are effectively “flowing” such that the system’s partition function remains invariant during the RG process. When we divide the action into fast and slow modes, the partition function becomes

$$\begin{aligned} Z &= \iiint D\theta'_{c<} D\theta_{f<} D\theta'_{c>} D\theta_{f>} e^{-S_{<}^{\text{eff}} - S_{>}^{\text{eff}} - S_I^{\text{eff}}} \\ &= \iint D\theta'_{c<} D\theta_{f<} e^{-S_{<}^{\text{eff}}} \iint D\theta'_{c>} D\theta_{f>} e^{-S_{>}^{\text{eff}}} e^{-S_I^{\text{eff}}} \\ &= \iint D\theta'_{c<} D\theta_{f<} e^{-S_{<}^{\text{eff}}} \langle e^{-S_I^{\text{eff}}} \rangle_{>}, \end{aligned} \quad (\text{S4})$$

where the expectation is calculated over all fast modes. Since the backscattering A is small, we approximate $\langle e^{-S_I^{\text{eff}}} \rangle > \approx e^{-\langle S_I^{\text{eff}} \rangle >}$, which can be calculated as

$$\begin{aligned} \langle S_I^{\text{eff}} \rangle > &= \iint D\theta'_{c>} D\theta_{f>} e^{-S_{>}^{\text{eff}}} \\ &\times A \int d\tau \cos \{2\sqrt{\pi} [\theta'_{c<}(\tau) + \theta'_{c>}(\tau)]\} \cos \{2\sqrt{\pi} [\theta_{f<}(\tau) + \theta_{f>}(\tau)]\} \\ &= \frac{A}{4} \sum_{\gamma, \eta=\pm 1} \int d\tau e^{i2\sqrt{\pi}[\gamma\theta'_{c<}+\eta\theta_{f<}]} \\ &\times \int D\theta'_c e^{-S_{c>}^{\text{eff}}} e^{i2\sqrt{\pi}\gamma \int_{>} \frac{d\omega}{2\pi} \theta'_c(\omega)} \int D\theta_f e^{-S_{f>}^{\text{eff}}} e^{i2\sqrt{\pi}\eta \int_{>} \frac{d\omega}{2\pi} \theta_f(\omega)}, \end{aligned} \quad (\text{S5})$$

where $S_{c>}^{\text{eff}} = \int_{\Lambda-d\Lambda < |\omega| < \Lambda} \frac{d\omega}{2\pi} [(1+r)|\theta'_c(\omega)|^2|\omega|]$ and $S_{f>}^{\text{eff}} = \int_{\Lambda-d\Lambda < |\omega| < \Lambda} \frac{d\omega}{2\pi} [|\theta_f(\omega)|^2|\omega|]$ are the fast-mode actions. These two integrals are standard Gaussian integrals so that

$$\begin{aligned} \langle S_I^{\text{eff}} \rangle > &= \frac{A}{4} \sum_{\gamma, \eta=\pm 1} \int d\tau e^{i2\sqrt{\pi}[\gamma\theta'_{c<}+\eta\theta_{f<}]} e^{-2\pi(1+\frac{1}{1+r}) \int_{\Lambda-d\Lambda}^{\Lambda} \frac{d\omega}{2\pi} \frac{1}{|\omega|}} \\ &= A e^{-(1+\frac{1}{1+r}) \frac{d\Lambda}{\Lambda}} \int d\tau \cos [2\sqrt{\pi}\theta'_c(\tau)] \cos [2\sqrt{\pi}\theta_f(\tau)]. \end{aligned} \quad (\text{S6})$$

Before we compare Eq. (S6) with the tunneling term in Eq. (S1) at the beginning of this section, we need to rescale the frequency as $\omega = \omega' \Lambda / (\Lambda + d\Lambda)$ such that the cutoff of ω' scales back to Λ . Consequently, to keep the partition function invariant, we have an effective backscattering strength A^{eff} which is related to the original A by

$$A^{\text{eff}} = A + dA = A e^{\frac{d\Lambda}{\Lambda} - (1+\frac{1}{1+r}) \frac{d\Lambda}{\Lambda}} \approx A - A \frac{1}{1+r} \frac{d\Lambda}{\Lambda}. \quad (\text{S7})$$

Now we choose the bandwidth D as the cutoff such that $dD = -d\Lambda$ and we have

$$\frac{dA}{d \ln D} = \frac{1}{1+r} A, \quad (\text{S8})$$

which is Eq. (23) in the main text.

II. DERIVATION OF DYNAMICAL COULOMB BLOCKADE (DCB) RESULT

In this section, we give a derivation of our result for the I - V curve, Eq. (30) in the main text, from DCB theory, following the classic DCB literature such as [S2–S5]. We start with the refermionized Hamiltonian Eq. (33) of the main text,

$$\begin{aligned} H' &= H_0 + H_r + H_{\text{bias}} \\ &= \frac{1}{2} \int_{-\infty}^{\infty} dx \left[\psi_R^\dagger(x) \partial_x \psi_R(x) - \psi_L^\dagger(x) \partial_x \psi_L(x) \right] + \pi a_0 A \cos [2\sqrt{\pi} \theta'_c(0)] \left[\psi_L^\dagger(0) \psi_R(0) + \text{h.c.} \right] \\ &+ \frac{eV}{2} \left[\int_{-\infty}^0 dx \psi_R^\dagger(x) \psi_R(x) - \int_0^{\infty} dx \psi_L^\dagger(x) \psi_L(x) \right], \end{aligned} \quad (\text{S9})$$

which describes two channels of chiral fermions and the environment-coupled tunneling between them. The backscattering Hamiltonian can be rewritten as a product of the bosonic and fermionic parts $H_r = H_r^B H_r^F$, with $H_r^B = \cos [2\sqrt{\pi} \theta'_c(0)]$. Using $|i\rangle$ and $|f\rangle$ to represent the initial and final states, we can calculate the rate of backscattering between those two states with Fermi's golden rule

$$W_{i \rightarrow f} = \frac{2\pi}{\hbar} |\langle f | H_r | i \rangle|^2 \delta(E_i - E_f). \quad (\text{S10})$$

To relate Eq. (S10) with macroscopic observables, we need to sum over possible initial and final states

$$\begin{aligned} \Gamma(V, T) &= \frac{2\pi}{\hbar} \int_{-\infty}^{+\infty} dE^i dE^f \sum_{R_1^i R_1^f} |\langle E^i | H_r^F | E^f \rangle|^2 |\langle R^i | H_r^B | R^f \rangle|^2 \\ &\times P_\beta(R^i) P_\beta(E) \delta(E^i + E_R^i + eV - E^f - E_R^f), \end{aligned} \quad (\text{S11})$$

where $|E^i\rangle$ represents the initial state of a quasi-particle in the right-moving channels with energy E^i , and $|E^f\rangle$ refers to the left-moving final state. As mentioned in the main text, θ'_c now functions as the dissipative bath, whose initial and final states are given by $|R^{i,f}\rangle$. Meanwhile, the initial density matrix element of bosonic states is described by $P_\beta(R^i) = \langle R^i | \rho_\beta | R^i \rangle$ (here β is a reminder that the density of states is thermally dependent). The fermionic statistics is described by $P_\beta(E)$ [see Eq. (S16) for details].

For later convenience, we rewrite the delta function in its integral form

$$\delta(E^i + E_R^i + eV - E^f - E_R^f) = \frac{1}{2\pi\hbar} \int_{-\infty}^{\infty} dt \exp \left[\frac{i}{\hbar} (E^i + E_R^i + eV - E^f - E_R^f) t \right]. \quad (\text{S12})$$

Combining the energy phase of the baths ($E_R^{i,f}$) with the corresponding matrix elements yields

$$\begin{aligned} & \sum_{R^i, R^f} |\langle R^f | \cos [2\sqrt{\pi}\theta'_c(0)] | R^i \rangle|^2 \cdot e^{\frac{i}{\hbar} (E_R^i - E_R^f) t} P_\beta(R^i) \\ &= \sum_{R^i, R^f} \langle R^i | \cos [2\sqrt{\pi}\theta'_c(t, 0)] | R^f \rangle \langle R^f | \cos [2\sqrt{\pi}\theta'_c(0, 0)] | R^i \rangle P_\beta(R^i) \\ &= \langle \cos [2\sqrt{\pi}\theta'_c(t, 0)] \cos [2\sqrt{\pi}\theta'_c(0, 0)] \rangle = \frac{1}{4} \left\langle e^{i2\sqrt{\pi}\theta'_c(t, 0)} e^{-i2\sqrt{\pi}\theta'_c(0, 0)} \right\rangle = \frac{1}{4} e^{J(t)}, \end{aligned} \quad (\text{S13})$$

where $J(t) \equiv 4\pi \langle [\theta'_c(t) - \theta'_c(0)] \theta'_c(0) \rangle$ is the phase-phase correlation function. In obtaining (S13), we used the relations [S2] $\langle e^{i\theta(t)} e^{i\theta(0)} \rangle = 0$ and

$$\langle e^{i2\sqrt{\pi}\alpha\theta(t)} e^{-i2\sqrt{\pi}\alpha\theta(0)} \rangle = e^{\alpha^2 4\pi \langle [\theta(t) - \theta(0)] \theta(0) \rangle} = e^{\alpha^2 J(t)}. \quad (\text{S14})$$

Since the free bosonic action is quadratic, we can calculate this correlation with a Gaussian integral [S2, S4]

$$J(t) = -\frac{2}{1+r} \ln \sinh\left(\frac{\pi k_B T |t|}{\hbar}\right) + \frac{2}{1+r} \ln \frac{\pi k_B T}{\hbar \omega_R} - \frac{2}{1+r} \frac{i\pi}{2} \text{Sign}(t) - \frac{2}{1+r} \gamma, \quad (\text{S15})$$

where ω_R is the energy cutoff of the bosonic bath and γ is Euler's constant.

Next we deal with the fermionic part. Based on the argument in the DCB method [S2], the backscattering barrier can be treated as an effective backscattering resistance R_T so that the fermionic matrix element can be rewritten as

$$|\langle E^i | H_r^F | E^f \rangle|^2 P_\beta(E) = \frac{\hbar}{2\pi e^2 R_T} f(E^i) [1 - f(E^f)], \quad (\text{S16})$$

where $f(E)$ represents the equilibrium Fermi-Dirac distribution.

Now combining the fermionic and bosonic parts and including the phase factor $\exp[i(E^i - E^f + eV)t/\hbar]$, we arrive at the expression for the backscattering rate

$$\begin{aligned} \Gamma(V, T) &= \frac{1}{2\pi\hbar e^2 R_T} \int_{-\infty}^{\infty} dE^i dE^f f(E^i) [1 - f(E^f + eV)] \int_{-\infty}^{+\infty} dt e^{J(t)} e^{\frac{i}{\hbar} (E^i - E^f) t} \\ &= \frac{1}{2\pi e^2 R_T} \frac{e^{\frac{eV}{2k_B T}}}{\Gamma(\frac{2}{1+r} + 2)} \left(\frac{2\pi k_B T}{\hbar \omega_R} \right)^{\frac{2}{1+r} + 1} \hbar \omega_R \left| \Gamma\left(\frac{1}{1+r} + 1 + i \frac{eV}{2\pi k_B T}\right) \right|^2. \end{aligned} \quad (\text{S17})$$

Physically, this backscattering rate only involves tunneling from the right-moving to left-moving channel; however, the “net” tunneling rate is described by the difference $\Gamma(V, T) - \Gamma(-V, T)$. Since the energy associated with the bias of each backscattering process is eV , we can reasonably argue that the charge carried by each quasi-particle is e . Consequently, the backscattering-related “current” is $\Delta I(V, T) = e [\Gamma(V, T) - \Gamma(-V, T)]$.

Meanwhile, from Eq. (S9) we know that when $A = 0$, the two fermionic chiral channels are decoupled, and the system attains a perfect conductance $G = e^2/h$. Thus we conclude that the current is

$$\begin{aligned} I(V, T) &= \frac{e^2}{h} V - \Delta I(V, T) \\ &= \frac{e^2}{h} V - e [\Gamma(V, T) - \Gamma(-V, T)] \\ &= \frac{e^2}{h} V - \frac{1}{R_T} \frac{1}{\Gamma(\frac{2}{1+r} + 2)} \left(\frac{2\pi k_B T}{\hbar \omega_R} \right)^{\frac{2}{1+r}} \times V \times \frac{|\Gamma(\frac{1}{1+r} + 1 + i \frac{eV}{2\pi k_B T})|^2}{|\Gamma(1 + i \frac{eV}{2\pi k_B T})|^2}, \end{aligned} \quad (\text{S18})$$

where we have used the equality $\sinh(\pi x) = \pi x \cdot \frac{1}{|\Gamma(1+ix)|^2}$. Eq. (S18) is just the current shown in the main text.

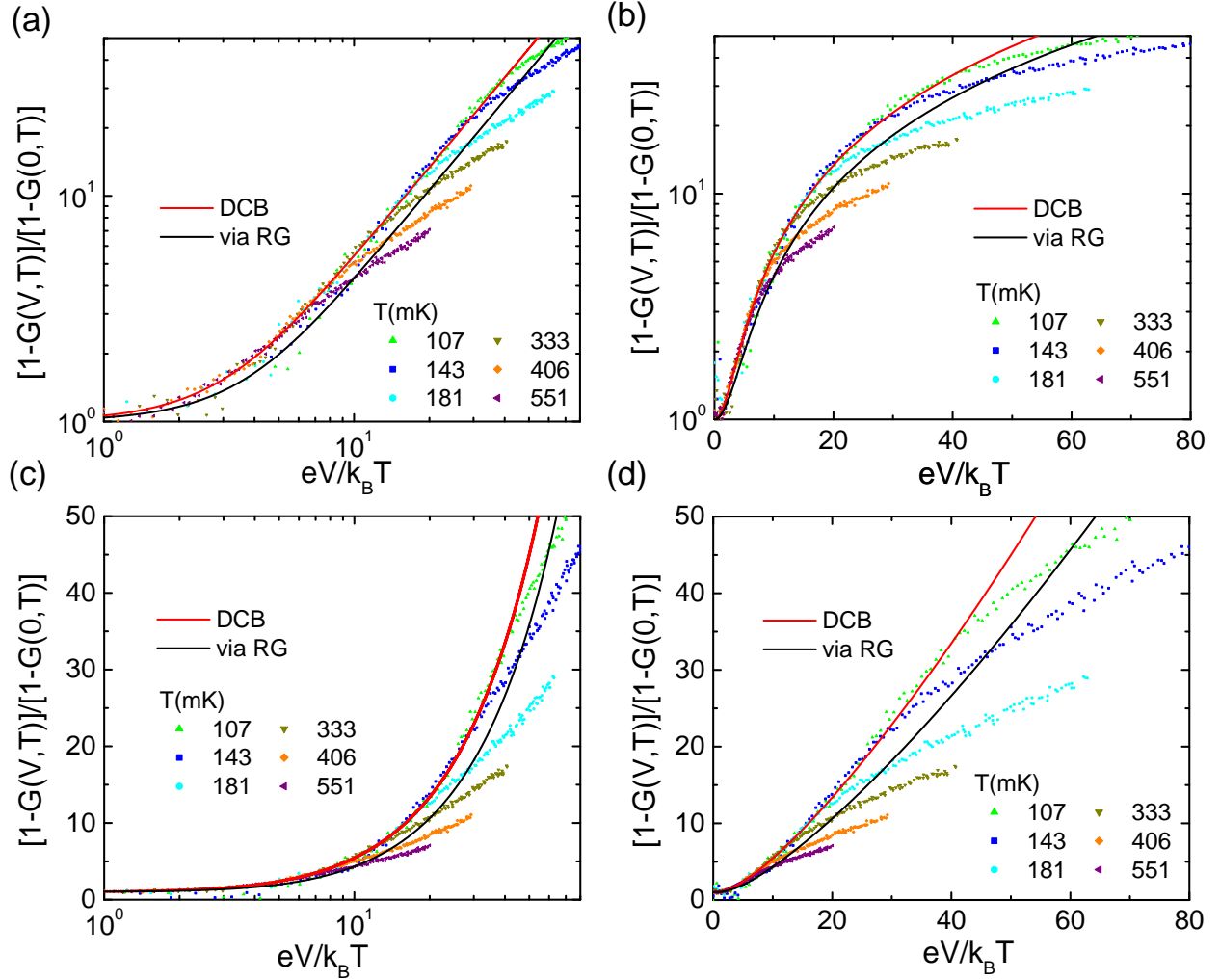


FIG. S1. Comparison between the experimental data and theoretical calculations with dissipation $r = 0.5$ [same data as in in Fig. 2(a) of main text]. We emphasize the excellent agreement of the DCB result with the experimental data in the crossover regime.

III. EXPERIMENTAL DATA OTHER THAN LOG-LOG PLOTS

To supplement the comparison between experimental data and the theoretical results, here we provide plots of the same data using different combinations of log and linear scales. Thus for the $r = 0.5$ case, in Fig. S1 we plot in four different ways the deviation of the differential conductance from perfect e^2/h : $[1 - G(V, T)]/[1 - G(0, T)]$ vs. $eV/k_B T$ is plotted on (a) log-log, (b) semi-log, (c) linear-log, and (d) linear-linear scales.

Focusing on the crossover regime, note the excellent agreement between the experimental data and theoretical results.

-
- [S1] Alexander Altland and Ben Simons, *Condensed Matter Field Theory* (Cambridge University Press, Cambridge, 2006).
 - [S2] G.-L. Ingold and Yu.V. Nazarov, “Charge tunneling rates in ultrasmall junctions,” in *Single Charge Tunneling: Coulomb Blockade Phenomena in Nanostructures*, edited by H. Grabert and M. H. Devoret (Plenum, New York, 1992) pp. 21–107, and arXiv:cond-mat/0508728.
 - [S3] Yu. V. Nazarov and Y. M. Blanter, *Quantum Transport: Introduction to Nanoscience* (Cambridge University Press, Cambridge, 2009).
 - [S4] M. Sassetti and U. Weiss, “Transport of 1d interacting electrons through barriers and effective tunnelling density of states,” *EPL (Europhysics Letters)* **27**, 311 (1994).
 - [S5] W. Zheng, J. R. Friedman, D. V. Averin, S. Y. Han, and J. E. Lukens, “Observation of strong Coulomb blockade in resistively isolated tunnel junctions,” *Sol. State Comm.* **108**, 839–843 (1998).